Design of a Robust Controller for an Unmanned Vehicle Based on Sliding Mode Theory

M. Noorollahzadegan[1], A. Vali[2], G. Derakhshan[3], H. Arasteh Rad[4], V. Behnamgol[5]

***Abstract*— In this paper, a sliding mode method is used to control an unmanned vehicle. The kinematics of simple bicycles is considered to control the system. Due to the nonlinear dynamics of the problem, the sliding mode method is used and the control system is designed to robust cross-sectional and continuous path perturbations. The control vector is designed for two subsystems simultaneously and computer simulations have been performed to evaluate the performance of the control system in two modes in the presence of cross-sectional and continuous path disturbances. In case of cross-sectional disturbances, it is shown that the position and angle of the vehicle follow the desired values with high accuracy. This issue is also reflected in the occurrence of continuous disturbances. The simulation results show the appropriate and acceptable performance of the control system.**

***Index Terms*— unmanned vehicle, sliding mode, nonlinear control, uncertainty.**

I. Introduction

ROAD accidents and traffic are among the issues that are considered internationally today. Recent advances to reduce these problems include unmanned vehicles technology [1]. In this technology, steering control is a very important issue. However, due to parametric uncertainties, automatic steering control can be problematic. For this reason, [2] presents an automatic vehicle controller based on model predictive control theory (MPC) that is robust to parametric uncertainties. In [3], the vehicle steering control is performed using the active disturbance rejection controller (ADRC). In this reference dynamic bicycle equations have been used. In [4], active disturbance rejection control is performed for automatic steering to keep the unmanned vehicle between the lines. The dynamic model used is a four-wheel dynamic model. The stability of the control system is proven based on Lyapunov theory. Predictive control for the steering system is performed in [5]. The used dynamic model is a two-wheeled model that focuses on the two front wheels of the car and their movements. In [6], the design of the state feedback control system for the steering has been done. The LPV problem and the combination of H_∞ method based on Lyapunov theory are also used in this reference. In [7], predictive sliding model control is proposed due to steering uncertainty. There are problems in finding the optimal route for each car so as to avoid collisions with other cars. For this purpose, in [8] a nonlinear model prediction controller (NMPC) is applied. Changing the line and preventing accidents for automatic vehicles is considered in [9]. In this paper, considering the kinematic model of bicycles for car steering and robust controller design is done. [10] examines the application of artificial intelligence technology in the field of unmanned vehicles for pedestrian detection. Active control simulation has been performed to prevent tractor overturning on road roughness in [11]. Robust control is provided for tracking a heavy vehicle in the [12]. Tracking and lateral stability is critical for heavy vehicles that are long. Proper performance due to the long length of the car and its variable mass requires different maneuvers. In addition, mass uncertainties and system performance against them are a significant challenge. H_∞ controller is used for this system. Estimation of tire slip angle in changing road conditions without knowing tire information to control vehicle stability in [13] has been done. In this reference, Kalman filter is used to estimate the slip angle of car tires. Reference [14] provides speed and position control of an unmanned vehicle using fuzzy logic.

In this paper, a MIMO sliding mode controller is designed to control the position and body angle of an unmanned vehicle using its kinematic model. Linear speed and steering angle are considered as two control inputs of this system. The proposed controller is designed as a vector due to the system model has two inputs and two outputs. In this case, the interactions between the two subsystems will also be considered. Also, continuous approximation method has been used to prevent chatting in the control signal. Another advantage of the controller used in this paper is the guarantee of finite time stability. The performance of this controller will be evaluated in the presence of two types of path disturbances. The goal is to track the desired position and angle.

In the second part, the simple dynamic model of the vehicle is modeled. In the third part, the controller design is done. Then, in the fourth section, by performing simulations, the performance of the control system is examined. Finally, a s conclusion will be provided.

Manuscript submitted Aug 4, 2021; revised Feb 5, 2022.

Mohsen Noorollahzadegan is a PhD candidate of the Islamic Azad University, Damavand, Iran (e-mail: M.nouri65@gmail.com).

Ahmadreza Vali is an Associate Professor of the Malek Ashtar University of Technology, Tehran, Iran (corresponding author to provide phone: 989121482603; e-mail: vali@mut.ac.ir).

Ghasem Derakhshan, is an Assistant Professor of the Islamic Azad University, Damavand, Iran, (e-mail: Gh.derakhshan@yahoo.com).

Hamid Arasteh Rad is an Assistant Professor of the Institute of Intelligent and Applied Systems, University Of Tehran, Tehran, Iran (e-mail: habib.arasteh@ut.ac.ir).

Vahid Behnamgol is an Assistant Professor of Malek Ashtar University of Technology, Tehran, Iran (e-mail: vahid_behnamgol@mut.ac.ir).

II. Dynamics Model

There are several models for studying the dynamic and kinematic behaviors of different types of vehicles. Bicycles dynamic and kinematic model are the most common and practical type (Figure 1). In order to simplify, in the kinematic model considered in this paper, movements such as roll, pitch or movement around the Z axis are not considered.

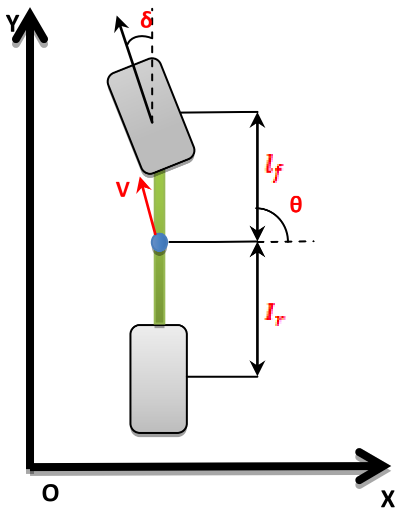

Fig. 1. Kinematic of the bicycle model [15]

The kinematic equations of the vehicle in the Cartesian coordinate system are as follows:

$$\begin{cases} \dot{X} = V \operatorname{Sin}\theta \\ \dot{Y} = V \operatorname{Cos}\theta \\ \dot{\theta} = \dfrac{V}{l_f} \times \operatorname{Tan}\delta \end{cases} \tag{1}$$

where X and Y shows the position of the vehicle, V linear speed, δ steering angle, θ the angle between the longitudinal axis of the vehicle and the X axis (body angle) and also l_f indicates the distance between the center of the vehicle axis and the center of the front wheel. The position of the vehicle and body angle as outputs can be controlled by control inputs $U_1 = V$ and $U_2 = \delta$ [15].

III. Controller Design

In this section, due to the nonlinearity of the system dynamics, by designing a sliding mode controller that is a nonlinear controller and is robust to uncertainties, The position of the vehicle (X, Y) and the angle of its body (θ) will be controlled by $U_1 = V$ and $U_2 = \delta$. The error vector, which represents the difference between the measured values and the desired values, is written as follows:

$$\begin{bmatrix} X_e \\ Y_e \\ \theta_e \end{bmatrix} = \begin{bmatrix} \operatorname{Cos}\theta_d & \operatorname{Sin}\theta_d & 0 \\ -\operatorname{Sin}\theta_d & \operatorname{Cos}\theta_d & 0 \\ 0 & 0 & 1 \end{bmatrix} * \begin{bmatrix} X - X_d \\ Y - Y_d \\ \theta - \theta_d \end{bmatrix} \tag{2}$$

That:

$$\begin{bmatrix} e_x \\ e_y \\ e_\theta \end{bmatrix} = \begin{bmatrix} X - X_d \\ Y - Y_d \\ \theta - \theta_d \end{bmatrix} \tag{3}$$

Error dynamics can be calculated as follows:

$$\begin{bmatrix} \dot{e}_x \\ \dot{e}_y \\ \dot{e}_\theta \end{bmatrix} = \begin{bmatrix} \dot{X} - \dot{X}_d \\ \dot{Y} - \dot{Y}_d \\ \dot{\theta} - \dot{\theta}_d \end{bmatrix} \tag{4}$$

By replacing (3) in (2), relation (5) is obtained:

$$\begin{bmatrix} X_e \\ Y_e \\ \theta_e \end{bmatrix} = \begin{bmatrix} e_x \operatorname{Cos}\theta_d + e_y \operatorname{Sin}\theta_d \\ -e_x \operatorname{Sin}\theta_d + e_y \operatorname{Cos}\theta_d \\ \theta - \theta_d \end{bmatrix} \tag{5}$$

To design a sliding mode controller, it is necessary to first define the sliding variables; So that the goal is to stabilize the sliding variables in a finite time. These variables vector has been selected as follows:

$$\begin{bmatrix} S_1 \\ S_2 \end{bmatrix} = \begin{bmatrix} X_e \\ K_1 Y_e + K_2 \theta_e \end{bmatrix} \tag{6}$$

The dynamics of sliding variables can be calculated as follow:

$$\begin{bmatrix} \dot{S}_1 \\ \dot{S}_2 \end{bmatrix} = \begin{bmatrix} \dot{X}_e \\ K_1 \dot{Y}_e + K_2 \dot{\theta}_e \end{bmatrix} \tag{7}$$

The error vector dynamics is derived from Equation (5) as follows:

$$\begin{bmatrix} \dot{X}_e \\ \dot{Y}_e \\ \dot{\theta}_e \end{bmatrix} = \begin{bmatrix} \dot{e}_x \operatorname{Cos}\theta_d - e_x \dot{\theta}_d \operatorname{Sin}\theta_d + \dot{e}_y \operatorname{Sin}\theta_d + e_y \dot{\theta}_d \operatorname{Cos}\theta_d \\ -\dot{e}_x \operatorname{Sin}\theta_d - e_x \dot{\theta}_d \operatorname{Cos}\theta_d + \dot{e}_y \operatorname{Cos}\theta_d - e_y \dot{\theta}_d \operatorname{Sin}\theta_d \\ \dot{e}_\theta \end{bmatrix} \tag{8}$$

By replacing (8) and (4) in (7) we can write:

$$\begin{bmatrix} \dot{S}_1 \\ \dot{S}_2 \end{bmatrix} = \begin{bmatrix} \dot{e}_x \operatorname{Cos}\theta_d - e_x \dot{\theta}_d \operatorname{Sin}\theta_d + \\ \dot{e}_y \operatorname{Sin}\theta_d + e_y \dot{\theta}_d \operatorname{Cos}\theta_d \\ K_1(-\dot{e}_x \operatorname{Sin}\theta_d - e_x \dot{\theta}_d \operatorname{Cos}\theta_d + \\ \dot{e}_y \operatorname{Cos}\theta_d - e_y \dot{\theta}_d \operatorname{Sin}\theta_d) + K_2 \dot{e}_\theta \end{bmatrix}$$

$$= \begin{bmatrix} (\dot{X} - \dot{X}_d)\operatorname{Cos}\theta_d - e_x \dot{\theta}_d \operatorname{Sin}\theta_d + \\ (\dot{Y} - \dot{Y}_d)\operatorname{Sin}\theta_d + e_y \dot{\theta}_d \operatorname{Cos}\theta_d \\ K_1(-(\dot{X} - \dot{X}_d)\operatorname{Sin}\theta_d - e_x \dot{\theta}_d \operatorname{Cos}\theta_d + \\ (\dot{Y} - \dot{Y}_d)\operatorname{Cos}\theta_d - e_y \dot{\theta}_d \operatorname{Sin}\theta_d) + K_2(\dot{\theta} - \dot{\theta}_d) \end{bmatrix} \tag{9}$$

Considering $U_2' = \dot{\theta} = \dfrac{V}{l_f} \times \operatorname{Tan}\delta$, we have:

$$\begin{bmatrix} \dot{S}_1 \\ \dot{S}_2 \end{bmatrix} =$$

$$\begin{bmatrix} U_1 \operatorname{Sin}\theta \operatorname{Cos}\theta_d - \dot{X}_d \operatorname{Cos}\theta_d - e_x \dot{\theta}_d \operatorname{Sin}\theta_d + \\ U_1 \operatorname{Cos}\theta \operatorname{Sin}\theta_d - \dot{Y}_d \operatorname{Sin}\theta_d + e_y \dot{\theta}_d \operatorname{Cos}\theta_d \\ K_1(-U_1 \operatorname{Sin}\theta \operatorname{Sin}\theta_d + \dot{X}_d \operatorname{Sin}\theta_d - e_x \dot{\theta}_d \operatorname{Cos}\theta_d + \\ U_1 \operatorname{Cos}\theta \operatorname{Cos}\theta_d - \dot{Y}_d \operatorname{Cos}\theta_d - e_y \dot{\theta}_d \operatorname{Sin}\theta_d) + K_2(U_2' - \dot{\theta}_d) \end{bmatrix} \tag{10}$$

We rewrite equation (10) as $\dot{S} = F + JU$,then:

$$\begin{bmatrix}\dot{S}_1\\ \dot{S}_2\end{bmatrix} = \begin{bmatrix} -\dot{X}_d \,\mathrm{Cos}\,\theta_d - e_x\dot{\theta}_d \,\mathrm{Sin}\,\theta_d - \dot{Y}_d \,\mathrm{Sin}\,\theta_d + e_y\dot{\theta}_d \,\mathrm{Cos}\,\theta_d \\ K_1(\dot{X}_d \,\mathrm{Sin}\,\theta_d - e_x\dot{\theta}_d \,\mathrm{Cos}\,\theta_d - \dot{Y}_d \,\mathrm{Cos}\,\theta_d - e_x\dot{\theta}_d \,\mathrm{Sin}\,\theta_d) - K_2\dot{\theta}_d \end{bmatrix} + \begin{bmatrix}\mathrm{Sin}\,\theta\,\mathrm{Cos}\,\theta_d & 0\\ K_1(\mathrm{Cos}\,\theta\,\mathrm{Cos}\,\theta_d - \mathrm{Sin}\,\theta\,\mathrm{Sin}\,\theta_d) & K_2\end{bmatrix} * \begin{bmatrix}U_1\\ U_2'\end{bmatrix} \tag{11}$$

The sliding mode controller consists of two parts; the first part is U_{equal} and is used to cancel certain sentences. The second part $U_{reaching}$ also ensures that the sliding variable reaches zero in a finite time. Therefore, the controller relation is determined as follows:

$$U' = \begin{bmatrix}U_1\\ U_2'\end{bmatrix} = J^{-1}(U_{equal} + U_{reaching}) \tag{12}$$

That:

$$U_{equal} = -F$$

$$U_{reaching} = v = \begin{bmatrix}v_1\\ v_2\end{bmatrix} = \begin{bmatrix}-K_1' Sign(S_1)\\ -K_2' Sign(S_1)\end{bmatrix} \tag{13}$$

$$J^{-1} = \begin{bmatrix} \dfrac{1}{\mathrm{Sin}\,\theta\,\mathrm{Cos}\,\theta_d + \mathrm{Cos}\,\theta\,\mathrm{Sin}\,\theta_d} & 0 \\ \dfrac{K_1(\mathrm{Sin}\,\theta\,\mathrm{Sin}\,\theta_d - \mathrm{Cos}\,\theta\,\mathrm{Cos}\,\theta_d)}{K_2(\mathrm{Sin}\,\theta\,\mathrm{Cos}\,\theta_d + \mathrm{Cos}\,\theta\,\mathrm{Sin}\,\theta_d)} & \dfrac{1}{K_2} \end{bmatrix} \tag{14}$$

Therefore, by replacing (13) and (14) in (12), we have:

$$U' = \begin{bmatrix}U_1\\ U_2'\end{bmatrix} = \begin{bmatrix} \dfrac{1}{\mathrm{Sin}\,\theta\,\mathrm{Cos}\,\theta_d + \mathrm{Cos}\,\theta\,\mathrm{Sin}\,\theta_d} & 0 \\ \dfrac{K_1(\mathrm{Sin}\,\theta\,\mathrm{Sin}\,\theta_d - \mathrm{Cos}\,\theta\,\mathrm{Cos}\,\theta_d)}{K_2(\mathrm{Sin}\,\theta\,\mathrm{Cos}\,\theta_d + \mathrm{Cos}\,\theta\,\mathrm{Sin}\,\theta_d)} & \dfrac{1}{K_2} \end{bmatrix} * \begin{bmatrix} \dot{X}_d \,\mathrm{Cos}\,\theta_d + e_x\dot{\theta}_d \,\mathrm{Sin}\,\theta_d + \dot{Y}_d \,\mathrm{Sin}\,\theta_d - e_y\dot{\theta}_d \,\mathrm{Cos}\,\theta_d - K_1' Sign(S_1) \\ -K_1(\dot{X}_d \,\mathrm{Sin}\,\theta_d - e_x\dot{\theta}_d \,\mathrm{Cos}\,\theta_d - \dot{Y}_d \,\mathrm{Cos}\,\theta_d - e_y\dot{\theta}_d \,\mathrm{Sin}\,\theta_d) + K_2\dot{\theta}_d - K_2' Sign(S_2) \end{bmatrix} \tag{15}$$

Finally:

$$U' = \begin{bmatrix}U_1\\ U_2'\end{bmatrix} = \begin{bmatrix} \dfrac{\dot{X}_d \,\mathrm{Cos}\,\theta_d + e_x\dot{\theta}_d \,\mathrm{Sin}\,\theta_d + \dot{Y}_d \,\mathrm{Sin}\,\theta_d - e_y\dot{\theta}_d \,\mathrm{Cos}\,\theta_d - K_1' Sign(S_1)}{\mathrm{Sin}\,\theta\,\mathrm{Cos}\,\theta_d + \mathrm{Cos}\,\theta\,\mathrm{Sin}\,\theta_d} \\ \dfrac{(K_1(\mathrm{Sin}\,\theta\,\mathrm{Sin}\,\theta_d - \mathrm{Cos}\,\theta\,\mathrm{Cos}\,\theta_d))\times(\dot{X}_d \,\mathrm{Cos}\,\theta_d + e_x\dot{\theta}_d \,\mathrm{Sin}\,\theta_d + \dot{Y}_d \,\mathrm{Sin}\,\theta_d - e_y\dot{\theta}_d \,\mathrm{Cos}\,\theta_d - K_1' Sign(S_1))}{K_2(\mathrm{Sin}\,\theta\,\mathrm{Cos}\,\theta_d + \mathrm{Cos}\,\theta\,\mathrm{Sin}\,\theta_d)} \end{bmatrix} + \begin{bmatrix} 0 \\ \dfrac{-K_1(\dot{X}_d \,\mathrm{Sin}\,\theta_d - e_x\dot{\theta}_d \,\mathrm{Cos}\,\theta_d - \dot{Y}_d \,\mathrm{Cos}\,\theta_d - e_y\dot{\theta}_d \,\mathrm{Sin}\,\theta_d) + K_2\dot{\theta}_d - K_2' Sign(S_2)}{K_2} \end{bmatrix} \tag{16}$$

According to equation (17) mentioned earlier:

$$U_2' = \dot{\theta} = \frac{V}{l_f} \times \mathrm{Tan}\,\delta \tag{17}$$

So, we get $U_2 = \delta$:

$$U_2 = \delta = \mathrm{Tan}^{-1}\left(\frac{U_2' \times l_f}{V}\right) \tag{18}$$

IV. Simulation Results

The control system is simulated in MATLAB software. The vehicle follows the desired closed route from the initial coordinates (0,0) along the axis X and Y at the specified desired angle.

A. Control system performance by applying cross-sectional road disturbances

In this case cross-sectional perturbation is considered. Then by applying V and δ, the performance of the controller and the effect of disturbances on the output are investigated. Figures 2 and 3 show the cross-sectional disturbances.

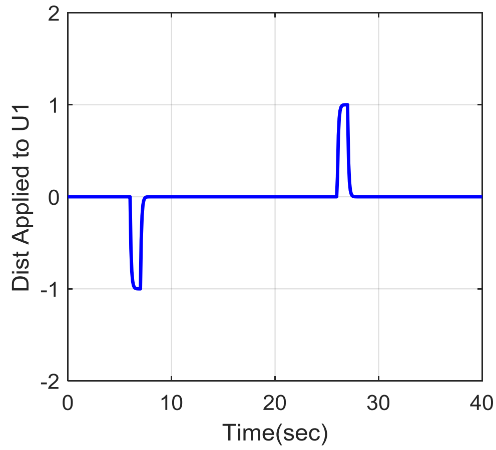

Figure 2. Disturbance entered to first control input

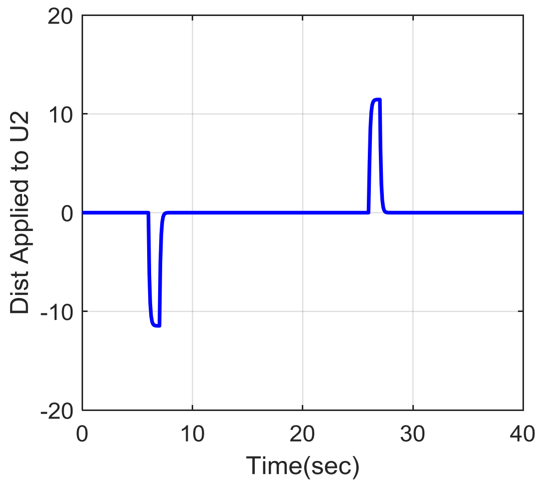

Figure 3. Disturbance entered to second control input

Figures 4 and 5 also show the linear velocity and steering angle diagrams, and it is expected that after applying them to the system, the desired route will be followed by the vehicle at the specified desired angle.

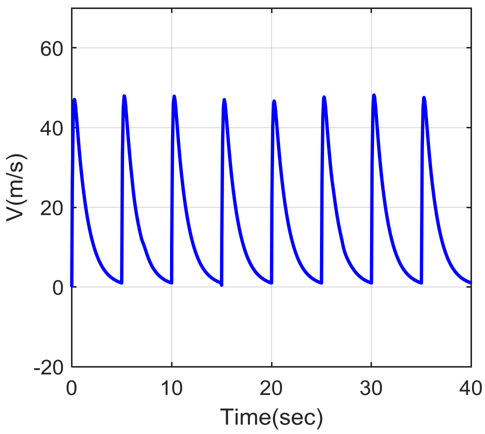

Figure 4- Linear velocity applied by vehicle (V)

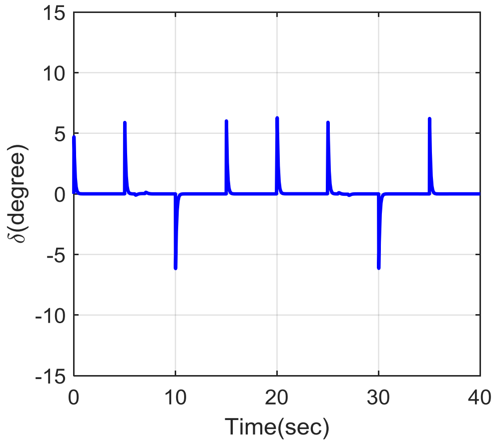

Figure 5. The steering angle applied to the vehicle (δ)

As shown in Figures 6 and 7, after applying V and δ by the vehicle, the desired path is determined with good accuracy and along this path, the body angle also corresponds to the desired body angle.

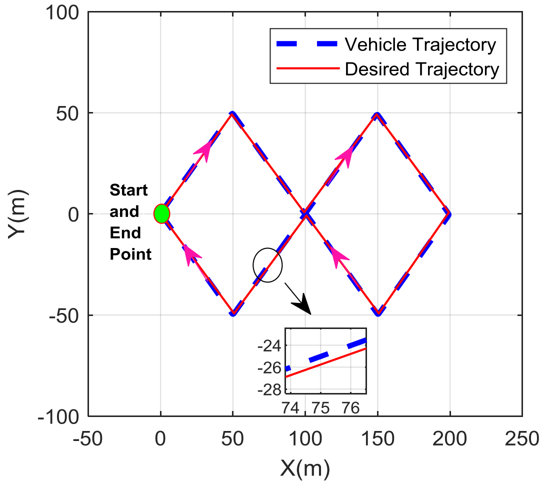

Figure 6- The vehicle path and the desired path

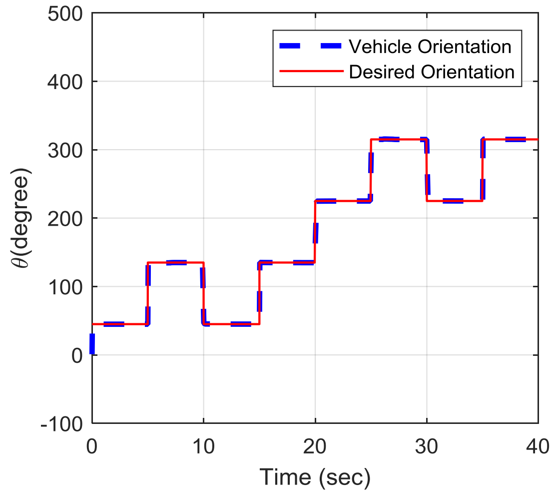

Figure 7- Body angle (θ) and its desired value

Figures 8 and 9 also show that the oscillations of the sliding variables occurred around zero and the designed controller performed well.

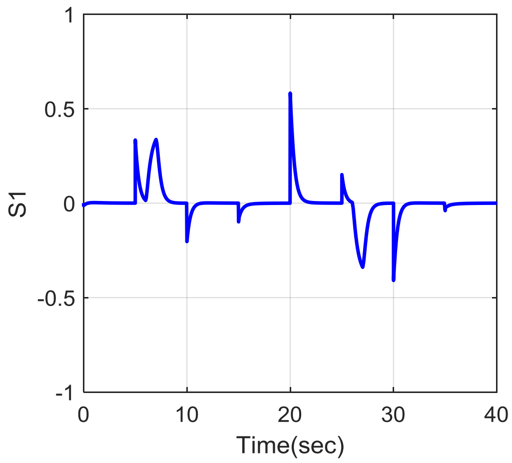

Figure 8- First sliding variable

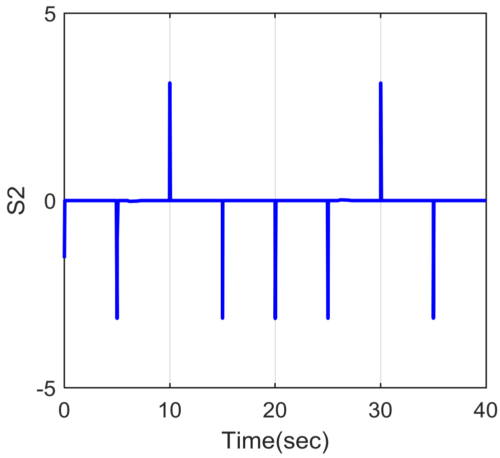

Figure 9 – Second sliding variable

According to the diagrams drawn, it can be concluded that the controller designed by sliding mode theory in the presence of disturbances is able to control the position and angle of the vehicle body, which shows the good performance of the controller and its robustness to disturbances.

B. Operation of the control system by applying continuous road disturbances

In this section in addition to U_1 and U_2, some uncertainties are added to X, Y and θ dynamics. Then V and δ calculated and by applying them to the vehicle, the performance of the controller is checked to control the position and angle of the vehicle body. Figures 10-12 show a diagram of the uncertainties.

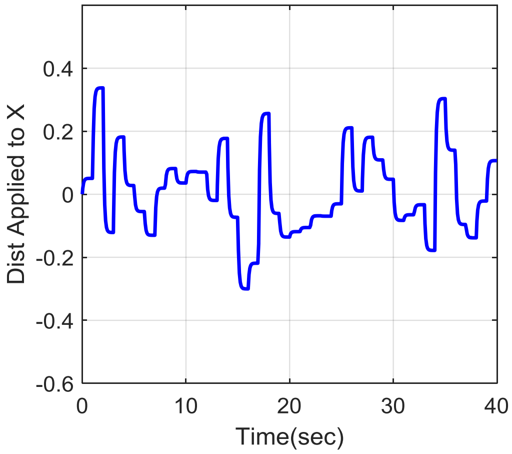

Figure 10 - Disturbance entered to X dynamic

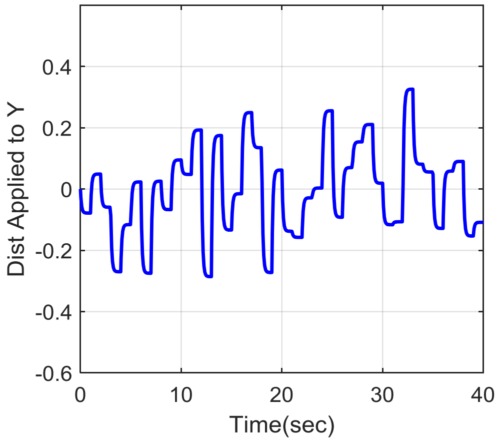

Figure 11 - Disturbance entered to Y dynamic

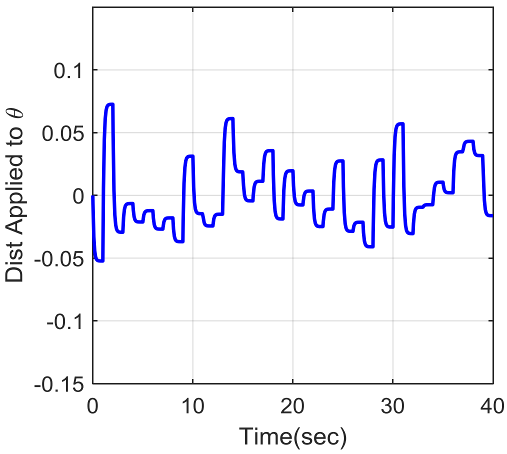

Figure 12 - Disturbance entered to θ dynamic

Figures 13 and 14 also show the uncertainties that have entered to inputs in this case.

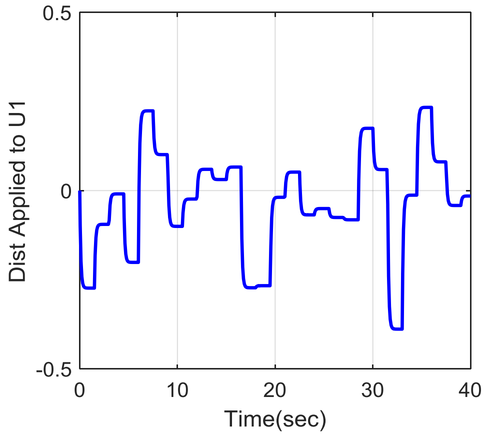

Figure 13 - Disturbance entered to first control input

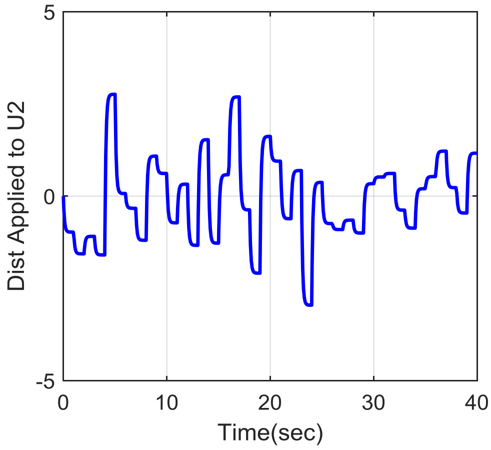

Figure 14 - Disturbance entered to second control input

Speed and steering angle are used to apply the vehicle, Figures 15 and 16 show their changes over time.

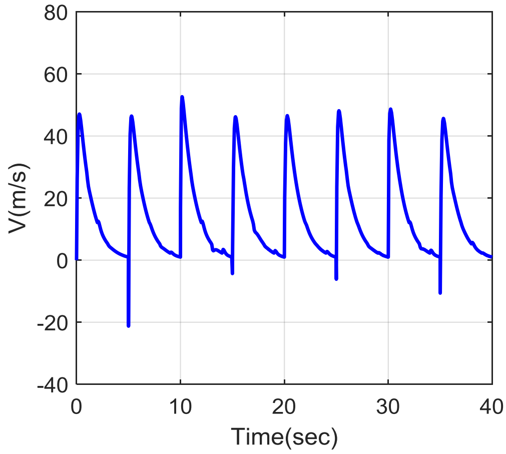

Figure 15 - Linear velocity applied by the vehicle (V)

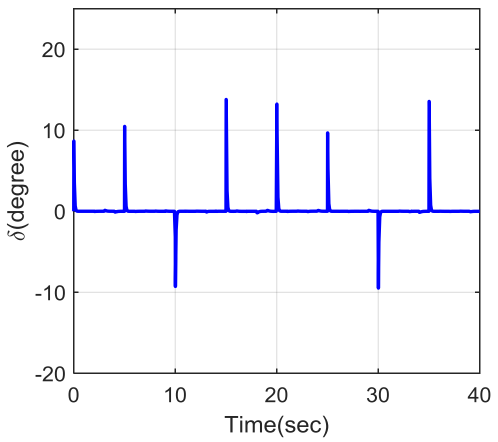

Figure 16- Steering angle applied by the vehicle (δ)

According to Figures 17 and 18, which show the route traveled and the angle of the vehicle body, it can be seen that the vehicle has been controlled by applying the speed and steering angle and has followed the desired values.

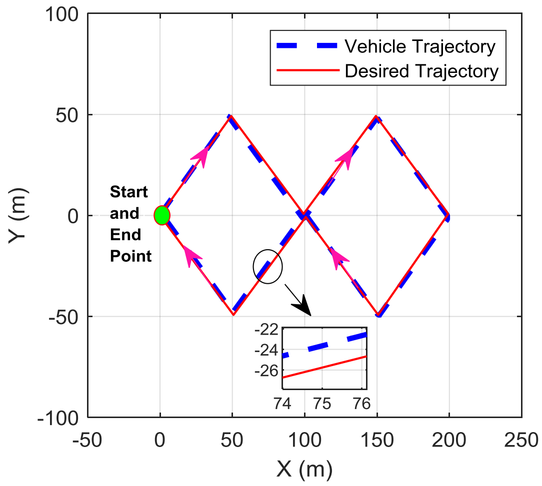

Figure 17 - The route traveled and the desired route in the two-dimensional page

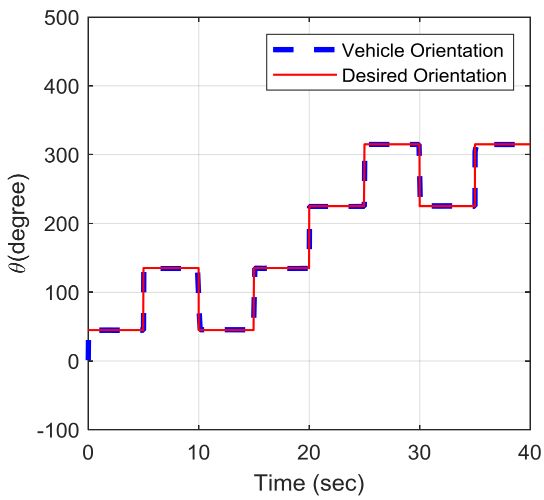

Figure 18- Body angle (θ) and its desired value

Figures 19 and 20 also show that the controller has acted well and changes S_1 and S_2 are around zero.

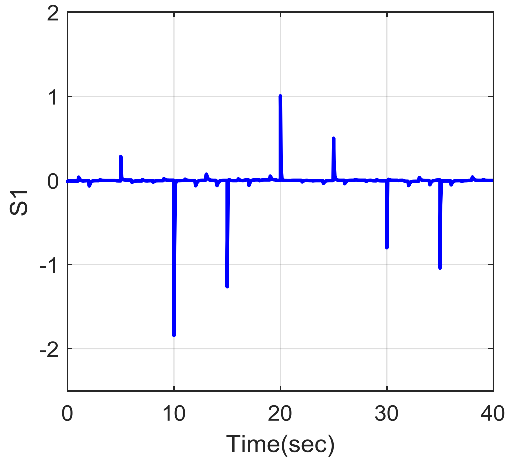

Figure 19 – First sliding variable

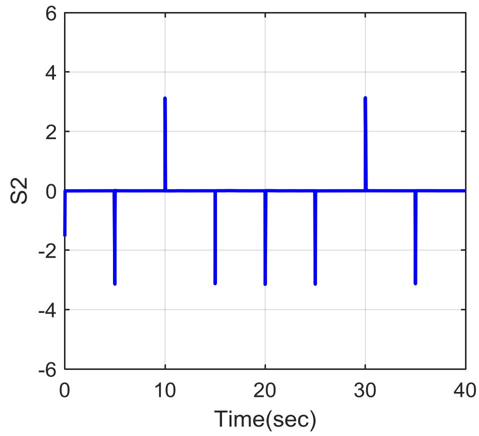

Figure 20 – Second sliding variable

In this approach, it is observed the position and angle of the vehicle body are controlled and the desired values are well tracked and the designed controller, against the disturbances, performed well.

C. Comparison of control system performance

In this section, the performance of the control system in the presence of cross-sectional and continuous disturbances is compared. In Figures 21, 22 and 23, error charts X, Y and θ is drawn, and in Table 1, the maximum and average error values are collected in the two desired cases.

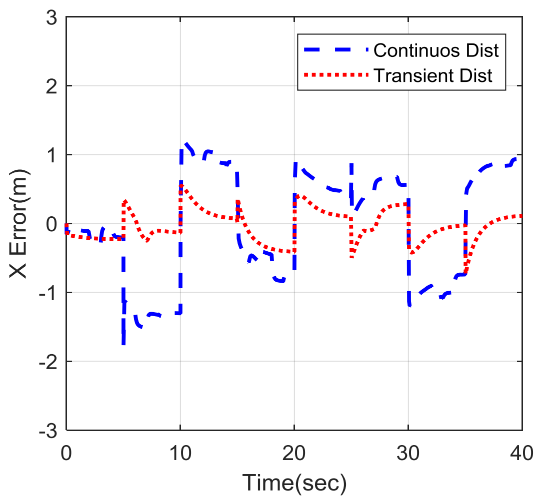

Figure 21 – error of X

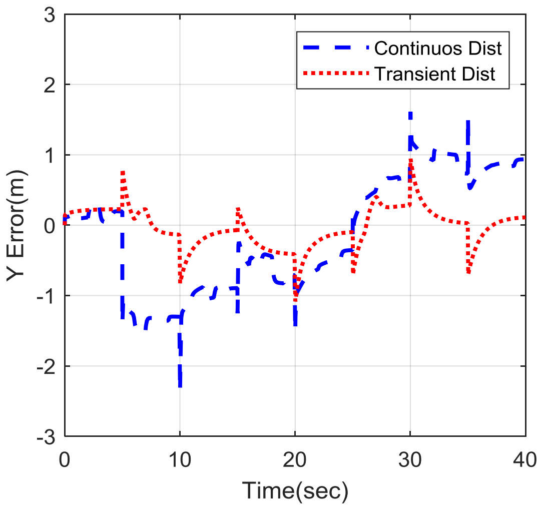

Figure 22 – error of Y

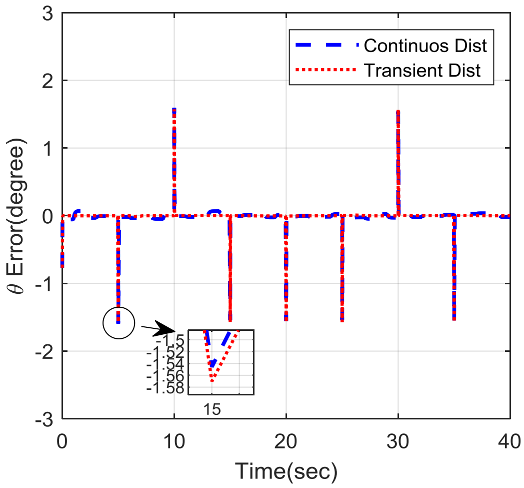

Figure 23 – error of θ

Table 1- Maximum size and average of error

continuous disturbances		cross-sectional disturbances		Error
Average of error	Maximum error	Average of error	Maximum error	
0.0366	17969	0.0355	0.734	error of X (m)
0.1292	2366	0.026	10828	error of Y (m)
0.0028	15931	0.0011	15736	error of θ (degree)

As it is clear from the results, in the application of cross-sectional disturbance, the maximum and average error is less and the car has followed the desired values with higher accuracy. However, it should be noted that the performance of the controller is acceptable in both cases and the car has followed the desired values with proper accuracy.

V. Conclusion

In this paper, a MIMO sliding model controller was designed based on the kinematic model of an unmanned vehicle. The purpose of the controller design is to control the position of the vehicle and the angle of its body. So that it follows the desired values specified for the position and angle of the body with appropriate accuracy. In the simulation section, the performance of the controller was evaluated in the presence of uncertainties in two approaches. In the first approach, cross-sectional perturbation was added to inputs. But in the second approach, some continuous type disturbances are added to state variables too. In both approaches, after calculating control input vector and applying them to the vehicle, it was observed that the path traveled by the vehicle as well as the body angle corresponded to the desired values and the controller in the presence of disturbances was well able to the control of the vehicle which was unmanned.

References

[1] Y. Amichai-Hamburger, et al. "The personal autonomous car: personality and the driverless car." *Cyberpsychology, Behavior, and Social Networking*, Vol. 23, No. 4, 2020, pp. 242-245.

[2] S. Cheng, et al. "Model-Predictive-Control-Based Path Tracking Controller of Autonomous Vehicle Considering Parametric Uncertainties and Velocity-Varying," *IEEE Transactions on Industrial Electronics*, Vol. 68, No. 9, 2021, pp. 8698-8707.

[3] L. Xiong, Y. Jiang, Z. Fu, "Steering Angle Control of Autonomous Vehicles Based on Active Disturbance Rejection Control", *IFAC Papers OnLine*, Vol. 51, No. 31, 2018, pp. 796–800.

[4] Z. Chu, et al. "Active disturbance rejection control applied to automated steering for lane keeping in autonomous vehicles", *Control Engineering Practice*, Vol. 74, 2018, pp. 13–21.

[5] A. Murilo, et al. "Design of a Parameterized Model Predictive Control for Electric Power Assisted Steering", *Control Engineering Practice*, Vol. 90, 2019, pp. 331–341.

[6] K. Yamamoto, et al. "Design and experimentation of an LPV extended state feedback control on Electric Power Steering systems", *Control Engineering Practice*, Vol. 90, 2019, pp. 123–132.

[7] D. Yang, et al. "A dynamic lane-changing trajectory planning model for automated vehicles", *Transportation Research Part C*, Vol. 95, 2018, pp. 228–247.

[8] A. Britzelmeier, and G. Matthias, "Non-linear model predictive control of connected, automatic cars in a road network using optimal control methods", *IFAC-Papers OnLine*, Vol. 51, No. 2, 2018, pp. 168-173.

[9] T. Peng, et al. "A new safe lane-change trajectory model and collision avoidance control method for automatic driving vehicles" *Expert Systems With Applications*, 2020.

[10] L. Liu, "Artificial Intelligence in the Field of Driverless Cars." *International conference on Big Data Analytics for Cyber-Physical-System*, Singapore, 2020.

[11] J. Qin, et al. "Simulation of active steering control for the prevention of tractor dynamic rollover on random road surfaces" *Bio Systems Engineering*, Vol. 185, 2019, pp. 135-149.

[12] F. M. Barbosa, et al. "Robust path-following control for articulated heavy-duty vehicles", *Control Engineering Practice*, Vol. 85, 2019, pp. 246–256.

[13] E. Joa, K. Yi, Y. Hyun, "Estimation of the tire slip angle under various road conditions without tire–road information for vehicle stability control", *Control Engineering Practice*, Vol. 86, 2019, pp. 129–143.

[14] J. Richard Navas, et al, "Fuzzy logic for speed control in object tracking inside a restricted area using a drone", *Developments and Advances in Defense and Security*, 2020, pp. 135-145.

[15] A. Baselga, E. Modelling, *planning and nonlinear control techniques for autonomous vehicles*, MS thesis. Universitat Politècnica de Catalunya, 2016.